Oceanologia, 15(1983)
PL ISSN 0078-3234

Jerzy OLSZEWSKI

Polish Academy of Sciences
Institute of Oceanology — Sopot

THE BASIC OPTICAL PROPERTIES OF THE WATER IN THE EZCURRA INLET*

1. INTRODUCTION

The results obtained during the Second Polish Antarctic Expedition, from vertical measurements of light transmission and irradiance of water in the Ezcurra Inlet have been analyzed in this paper. The measurements were conducted from 20th December 1977 through 10th March 1978, on board a vessel anchored at a given point with a depth of about 70 to 80 m. Three wave-lengths in the visible band were chosen with the aid of narrow interference filter. Parallel measurements at lengths of 525 and 425 nanometers were carried out in the first period of investigations (20th December to 4th February), while wave-lengths of 525 and 600 nanometers were employed throughout the second part of the study (4th February to 10th March).

Transmission measurements, used to determine the beam attenuation coefficient, were conducted using a standard single-beam transmission probe [11], with an $l_0=1$ m optical path in water. Continuous transmission profiles were analogue-recorded during vertical sounding in the depth range of 0 through 70 m. Two consecutive measurements were usually conducted, with respective filters, for two wave-lengths. The device was calibrated with water, twice distilled and filtered. The resultant absolute error of measurements, as the total of calibration and joint instability of the source of light and receiving unit did not exceed 0.05 m^{-1}, giving a fairly high relative error of 30% for extremely small values of the coefficient, correspondingly decreasing with their increase.

Measurements of irradiance, used to determine the coefficient of

* These studies were carried out under the research program MR II 16 coordinated by the Institute of Ecology of the Polish Academy of Sciences. They were sponsored in part under research program MR I 15 coordinated by the Institute of Hydro-Engineering of the Polish Academy of Sciences.

diffusive attenuation of light, were carried out with two standard irradiance meters [11], coupled at one level, which receive light with two wave-lengths simultaneously. In this case, recording was digital, by means of fast photocurrent integrators, with arbitrary depth steps (usually 1-m at the surface and 5-m at lower depths). The measurement error was mostly due to the vessel's hull (shadows or reflection), deviation of the axis of the meter from the vertical line caused by the vessel's drifting around its anchor, fluctuations of underwater illumination (the time of photocurrent averaging at single depth was short, ± ten seconds — due to the necessity to save time during measurements), and changes in external light, partially eliminated by simultaneous measurements of illumination above the water surface, always at wave-lengths corresponding to the underwater illumination. The resulting relative error of measurements can be estimated as 20% of the measured irradiance.

Because of the considerable and irregular variability of the measured parameters, it was inexpedient to analyze their instantaneous values. Similarly, when searching for relationship between these parameters one has to refrain from looking for direct functional relations, mainly because both places and times of measurements of different quantities were not identical, due to the vessel drifting and the quantities being measured one after the other, with as much as one-hour time intervals. Thus, the only possibility was to use statistical analysis, with its mean value and statistical correlations. Except for a few specially planned diurnal measurements of transmission, 10 days (240 hours) were taken as the shortest period of averaging. It was only this type of analysis which afforded a certain image of the optical properties of the investigated medium, acceptable as the average during the period of investigations; to what extent typical, however, would require observations lasting several years. One can only assume with caution that the situation presented here is fairly typical for the summer season in the coastal zone of a small water body, such as a fiord, surrounded by a glacier, and with a limited inflow of oceanic water.

2. LIGHT BEAM ATTENUATION

The beam attenuation coefficient c, (the sum of the coefficients of absorption and scattering, a and b, respectively) was taken as the parameter characterizing light attenuation in the investigated environment. This coefficient is one of the basic inherent optical properties of water [6], which enables the determination of such optical derivatives as transmission T of a collimated beam of light over a certain distance, l,

and the visibility range r, defined as the horizontal range of detection of an ideal black disk by a detector (eye) with a threshold sensitivity of 0.02 [2, 9]. The relations for the above parameters are:

$$T = \exp(-cl) \qquad r = \frac{\log 50}{c} \tag{1}$$

The coefficients c found for wavelengths of 425, 525 and 600 nanometers at selected depths are shown in Tables 1, 2 and 3, the values of c_w for the distilled water used for calibration, were taken from paper [4] as follows:

$$c_w(425)=0.0429, \qquad c_w(525)=0.0334, \qquad c_w(600)=0.2294$$

The variability of the attenuation coefficient was analyzed for the 525-nanometer wavelength (Table 1), which yields the extreme (minimum) value of c, as this is in the best light transmission band in the waters investigated.

Examples of typical vertical profiles of the coefficient of attenuation are given in Fig. 1. The profiles were taken every six hours from series of hourly measurements round-the-clock on 17th and 18th January 1978.

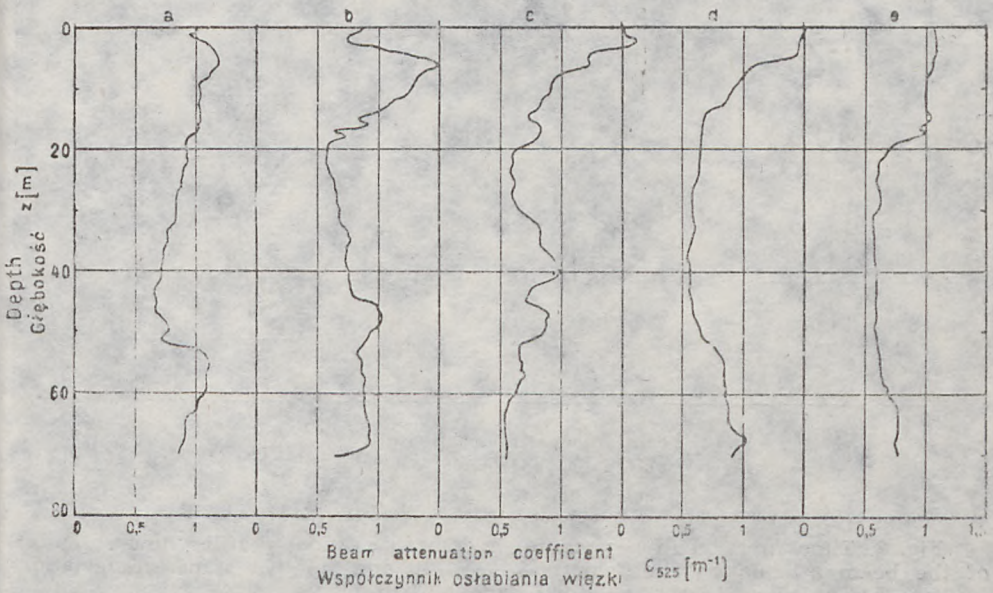

Fig. 1. Vertical profiles of the beam attenuation coefficient for the 525 nm light wavelength, measured during 24-hour observations on 17—18 January 1978:
17 I: *a* — 11.00 GMT, *b* — 17.00 GMT, *c* — 23.00 GMT,
18 I: *d* — 05.00 GMT, *e* — 11.00 GMT

Rys. 1. Profile pionowe współczynnika osłabiania wiązki promieni dla długości fali świetlnej 525 nm, zmierzone podczas stacji dobowej 17—18 I 1978

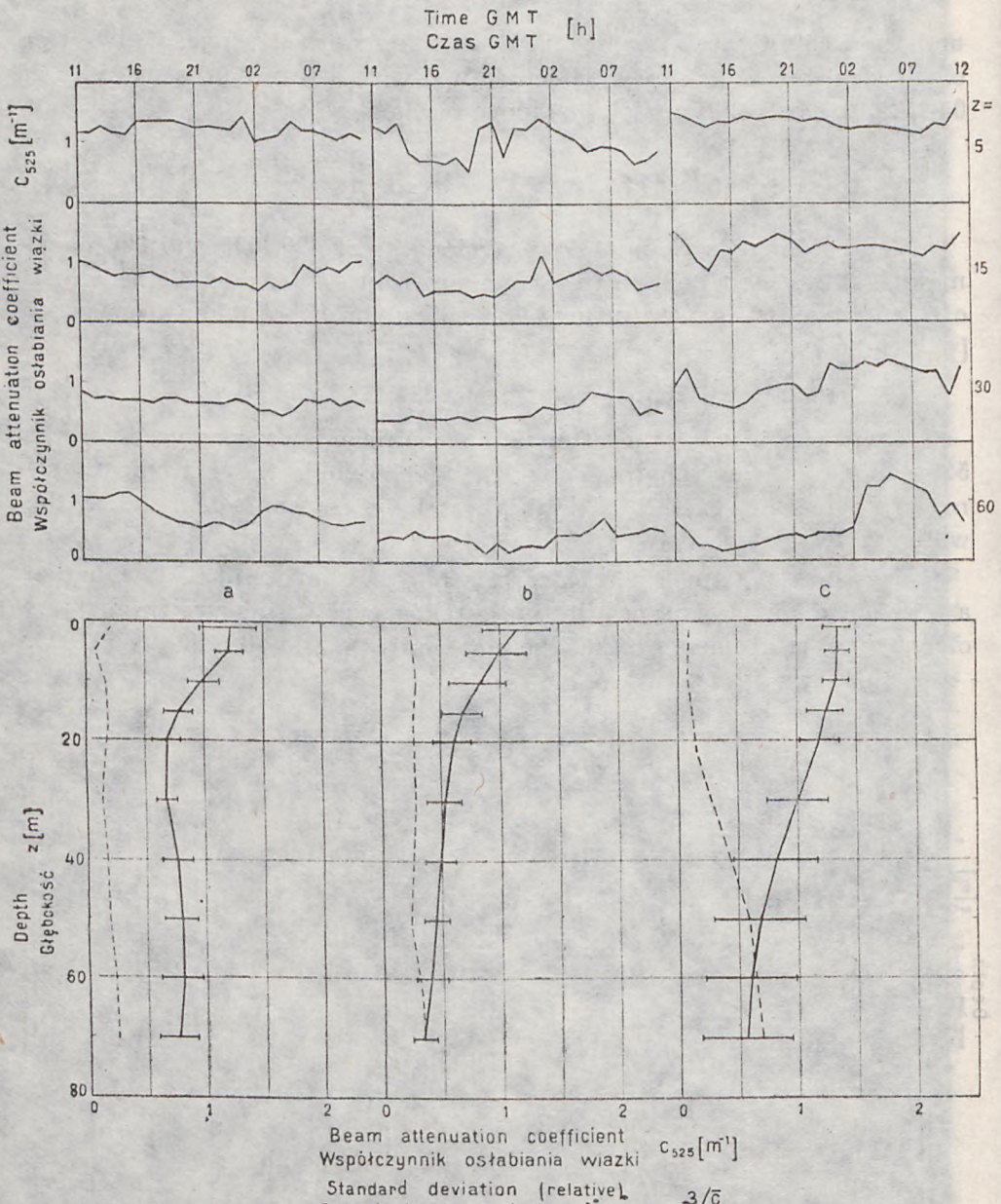

Fig. 2. Time function (upper figure) and mean vertical profiles (lower figure) of the beam attenuation coefficient (————), and relative standard deviation (- - - - - -) at selected depths, obtained from measurements during 24 hour observations for the 525 nm light wavelength: *a* — 17—18 January, *b* — 3—4 February; *c* — 17—18 February 1978

Rys. 2. Przebieg czasowy (rys. górny) i średnie profile pionowe (rys. dolny) współczynnika osłabiania wiązki promieni (————) i względnego odchylenia standardowego (- - - - - -) na wybranych głębokościach, znalezione dla długości fali świetlnej 525 nm na podstawie pomiarów poczas stacji dobowych: *a* — 17—18 I; *b* — 3—4 II; *c* — 17—18 II 1978

The temporal variation of the coefficient at depths of 5, 15, 30 and 60 m is presented in Fig. 2, which also contains the c-data for two other hourly series on 3 to 4 February and 17 to 18 February 1978. In order to facilitate comparison, all values in the drawing are reduced to the wavelength of 525 nanometer (by the formulae given below). In all cases illustrated in Fig. 2 the time series are highly irregular. However, signs of cyclic behaviour with a period of about 12 hours, likely to be coupled with tides, appear to be present in the series for lower depths.

The lower part of Fig. 2 shows vertical profiles of the coefficient c obtained from the three measurement series mentioned, averaged over 24 hours. A certain tendency can be noted in these profiles. In all three cases the highest values of c are observed just beneath the water surface a monotonic decrease with depth being pronounced in two cases, (*b*) and (*c*). A local minimum of the mean coefficient of attenuation at depths of about 20 to 30 m was found in case (*a*). The standard deviations, shown in the drawing with diagonal lines, and their relative values (broken line) suggest that the fluctuations of c increase with depth, especially in case (c); in case (*a*), again their behaviour is different, as c varies most near the surface and near the bottom (60 to 70 m), while a fairly distinct

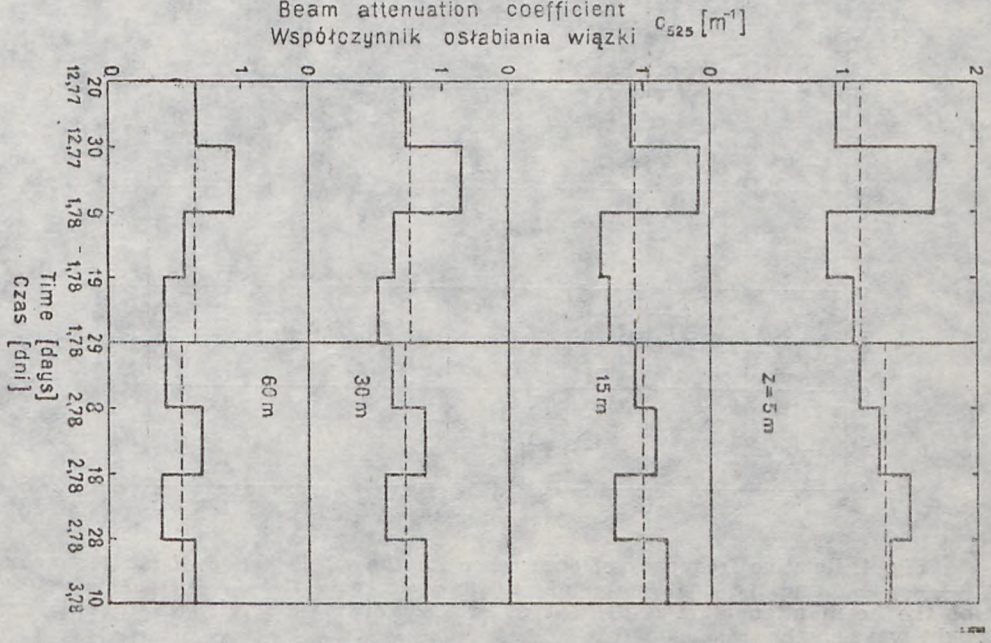

Fig. 3. Time function of the values of the beam attenuation coefficient at selected depths, averaged over 10-day (————) and 40-day (- - - - -) periods for the 525 nm light wavelength

Rys. 3. Przebieg czasowy uśrednianych w odcinkach 10-dniowych (————) i 40-dniowych (- - - - -) wartości współczynnika osłabiania wiązki promieni na wybranych głębokościach, dla długości fali świetlnej 525 nm

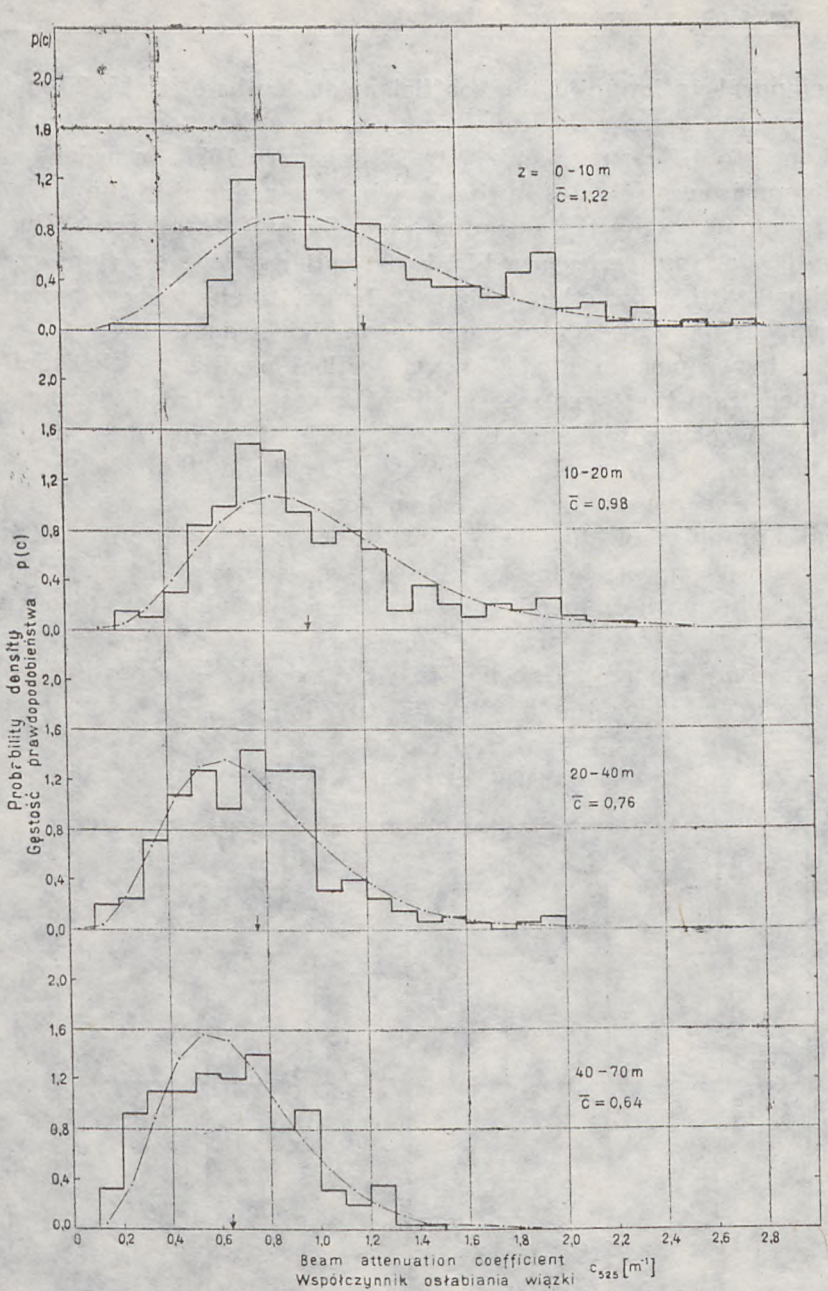

Fig. 4. Relative frequency of occurrence for the whole period of measurements (————), and the distribution of probability density (- - - - - - -), of the values of the beam attenuation coefficient at selected depth intervals, for the 525 nm light wavelength

Mean values are indicated by vertical arrows.

Rys. 4. Znaleziona dla całego okresu pomiarów względna częstość występowania (————) i rozkład gęstości prawdopodobieństwa (- - - - - - -) wartości współczynnika osłabiania wiązki promieni w wybranych przedziałach głębokości, dla długości fali świetlnej 525 nm

Pionową strzałką zaznaczono wartości średnie.

minimum occurs around the depth of 5 m. As will be shown further, case (*a*) still appears closest to the average variation, while cases (*b*) and (*c*) have the most probable *c*-profiles.

Fig. 1 and 2 give examples of short-term variation of the coefficient of attenuation in the studied environment. Fig. 3 illustrates the variation of this coefficient in time at depths of 5, 15, 30 and 60 m, averaged over a ten-day period. Since these measurements were carried out only once, it is impossible to compare the data of Fig. 3 with typical curves. In particular one does not know if the strong maximum of *c*, found in the second decade of the measurements (1977-12-30 through 1978-1-9) is typical. Further averaging, indicated by a broken line, for the first and second parts of the measurements, 1977-12-29 through 1978-1-29 and 1978-1-30 through 1978-3-10, shows a fairly characteristic tendency (should this be confirmed by data from a period of many yers). Compared with the first half, the second half displays higher coefficients of attenuation in the surface layer (5 and 15 m) and a decrease at lower depths (30 and 60 m).

The consecutive figures contain data obtained over the entire period of measurements. Fig. 4 presents distributions of the relative frequency of *c* in steps of 0.1 m^{-1} and averaged over four depth intervals: 0 to 10 m, 10 to 20 m, 20 to 40 m and 40 to 70 m. Distributions of these frequencies can be approximated with the Γ-type probability density function

$$p(c) = \frac{\beta^{\alpha}}{\Gamma(\alpha)} c^{\alpha-1} e^{-\beta c} \qquad (2)$$

in which

$$\alpha = \frac{\bar{c}^2}{\sigma^2}$$

$$\beta = \frac{\bar{c}}{\sigma^2}$$

and the distribution parameters found from the frequency corve are:

$\bar{c}$ = 1.224 / mean value / ; σ^2 = 0.2216 / variance, for depths of 0 to 10 m

$\bar{c}$ = 0.977 " ; σ^2 = 0.1575 " " " " 10 to 20 m

$\bar{c}$ = 0.755 " ; σ^2 = 0.1018 " " " " 20 to 40 m

$\bar{c}$ = 0.642 " ; σ^2 = 0.0759 " " " " 40 to 70 m

The following properties of the distribution were observed with increasing depth:

1° — continuous decrease in mean value,

2° — continuous decrease in variance,

3° — decrease in the difference between the mean value and the most probable value.

These properties are confirmed by the next figure, in which vertical profiles are given for mean values, most probable values and standard deviations of the coefficient of attenuation, averaged over the entire period of measurements, every 5 m close to the surface and every 10 m below. The profile of mean value shows a decrease in c, from 0 to 20 or 30 m, a smooth course with a slight minimum at 60 m and a minor increase close to the bottom. The standard deviation, shown with diagonal lines, also decreases with depth, but the relative deviation (broken line) is not so clear, with its local maxima and minima, of which the lowest occurs close to the surface (5 to 10 m). A similar low scatter of c is observed at the very bottom (70 m). The primary maximum of all relative deviations occurs at 60 m. This behaviour suggests that the water is most dynamically stable just beneath the surface (even though at a certain proximity) and close to the bottom, while the lowest stability is found about 10 to 20 m above sea bottom.

Fig. 5 also includes profiles of light transmission in a 1-m water layer, averaged over the entire period of measurements, together with the profiles of the horizontal range of visibility, computed by formulae (1). In accordance with the coefficient of attenuation, the lowest values of transmission, T, (26%), and range of visibility, r (2,9 m) occur at the surface, while the highest values can be found in the bottom layer, having a thickness about 30 m ($T=53\%$, $r=6.1$ m).

Let us now dwell on the relationship between the coefficients of attenuation measured for the three wavelengths mentioned above (425, 525 and 600 nm). Figures 6 and 7 present the sets of the coefficients c measured almost simultaneously for 525 and 425 nm (Fig. 6) and 525 and 600 nm (Fig. 7). In both cases, the least-squares analysis of the measured values gives an almost linear (with correlation factor close to unity) relationship between the coefficients for 425 and 600 nm and that measured in 525-nm waves. The computed equations of linear regression are

$$c_{425}=(1.173\pm0.022)\,c_{525}+(0.006\pm0.022)$$

with coefficient of correlation $\varrho=0.95$, (3)

$$c_{600}=(0.946\pm0.033)\,c_{525}+(0.223\pm0.034)$$

with coefficient of correlation $\varrho=0.89$. The „plus or minus" sign is given for the standard deviations of the coefficients in the equations.

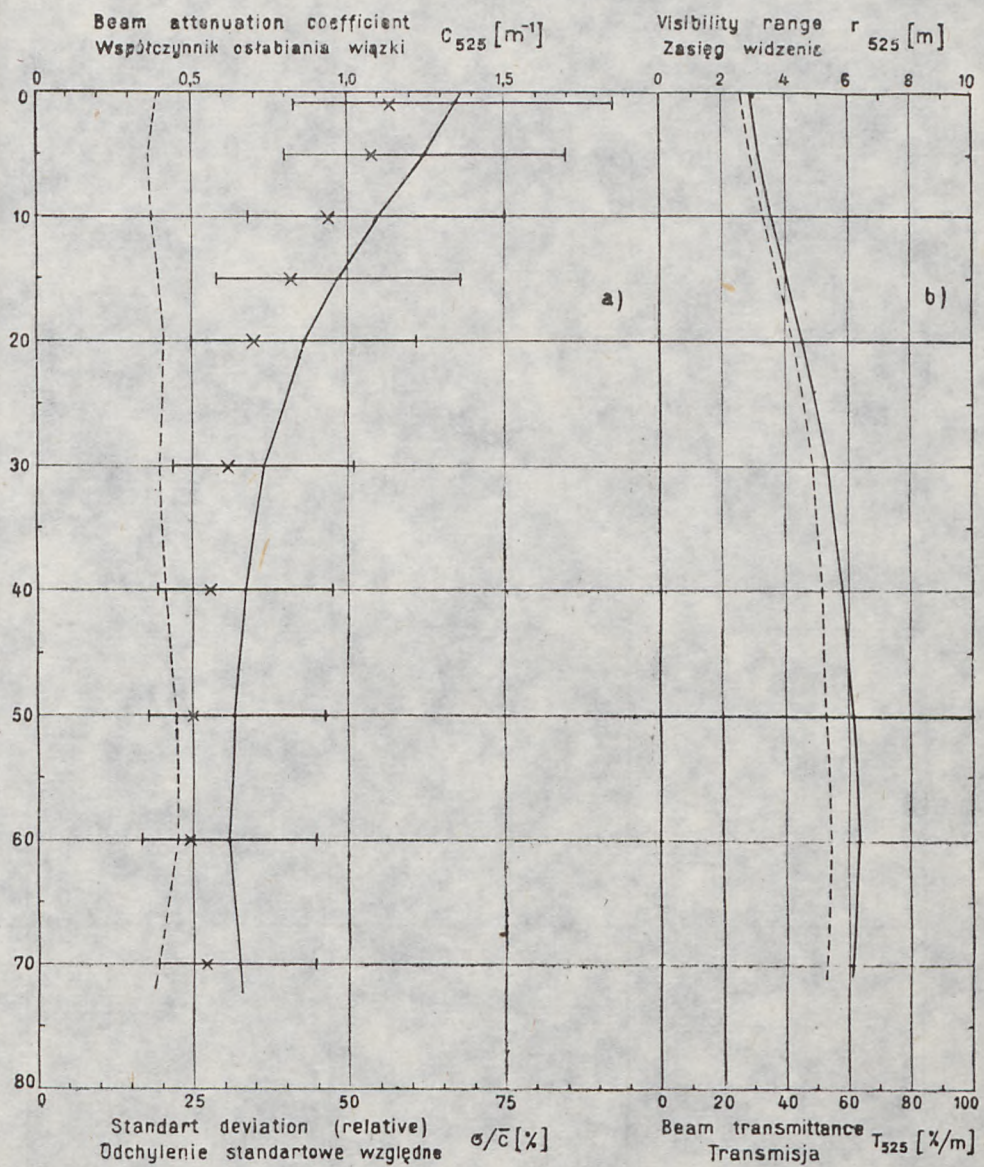

Fig. 5. Vertical profile of the beam attenuation coefficient (*a*: ———), relative standard deviation (*a*: - - - - - -), range of visibility (*b*: ———) and transmission (*b*: - - - - -), all averaged over the period of measurements for the 525 nm light wavelength

Crosses indicate the most probable values.

Rys. 5. Uśredniony w całym okresie pomiarów profil pionowy współczynnika osłabiania wiązki promieni (*a*: ———), względnego odchylenia standardowego (*a*: - - - - - -), zasięgu widzenia (*b*: ———) i transmisji (*b*: - - - - -), dla długości fali świetlnej 525 nm

Krzyżykami zaznaczone są wartości najbardziej prawdopodobne.

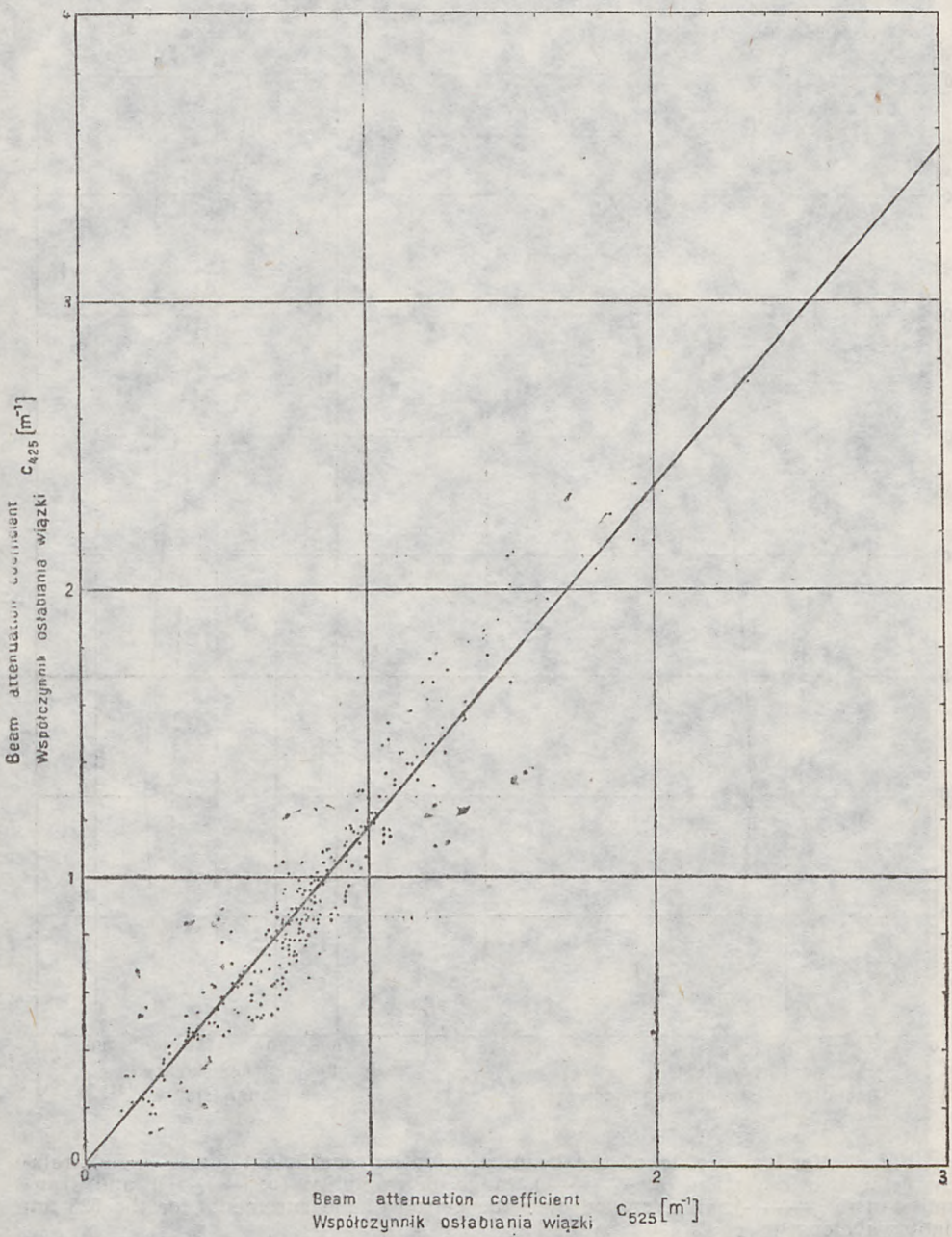

Fig. 6. Set of experimental points and regression line, determining the dependence of the beam attenuation coefficient for the 425 nm light wavelength on the coefficient for 525 nm

Rys. 6. Zbiór punktów pomiarowych i linia regresji określające zależność współczynnika osłabiania wiązki promieni dla długości fali świetlnej 425 nm od współczynnika dla 525 nm

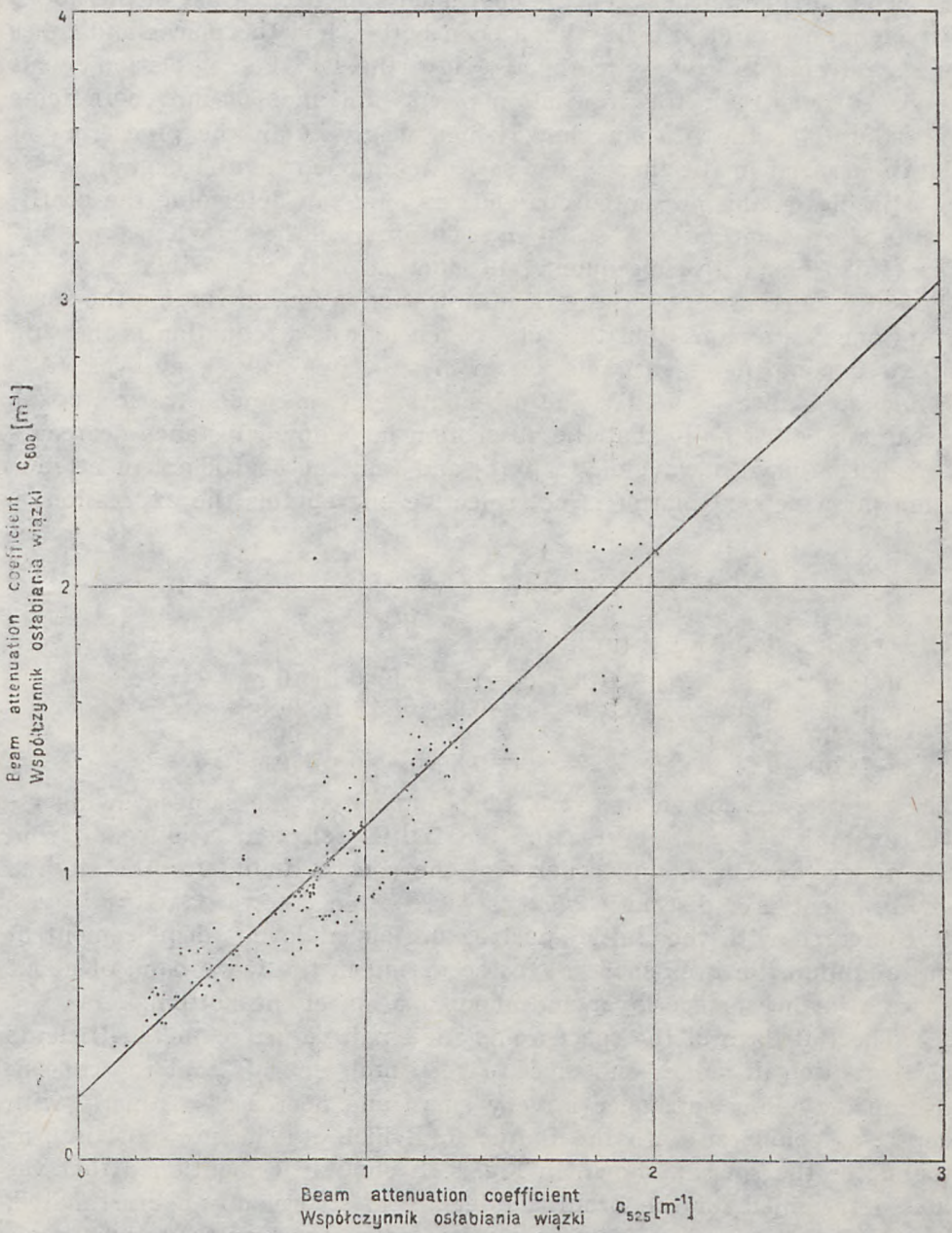

Fig. 7. Set of experimental points and regression line, determining the dependence of the beam attenuation coefficient for the 600 nm light wavelength on the coefficient for 525 nm

Rys. 7. Zbiór punktów pomiarowych i linia regresji określające zależność współczynnika osłabiania wiązki promieni dla długości fali świetlnej 600 nm od współczynnika dla 525 nm

The correlation between the coefficients of attenuation in the above wavelengths would probably have been better, had the places and times of measurements been synchronous. Nevertheless, the correlation seems to be sufficient for the translation of 425-nm and 600-nm coefficients into those for the 525-nm band, which was used in the processing of data measured in the three daily series mentioned at the beginning.

Basing on the presented correlations, one can determine the coefficients of attenuation for $\lambda = 425$ and 600-nm from the known mean values for $\lambda = 525$ nm, with subsequent reproduction of an approximate from of the entire spectrum of the coefficient of attenuation. In finding the spectrum one can assume that the total coefficient of attenuation is the sum of three components: attenuation in clear water, $c_w(\lambda)$, absorption in yellow substance [7], $a_y(\lambda)$, and attenuation in suspended matter, $c_p(\lambda)$. Assuming additionally that the absorption in yellow substance decreases exponentially with wavelength [6, 8] and that the coefficient of attenuation in suspended matter is not selective one obtains the expression:

$$c(\lambda) = c_w(\lambda) + a_y(425)\, e^{-k(\lambda - 425)} + c_p \qquad (4)$$

The coefficients of Eq. 4 (in m^{-1}) are:

$a_y(425) = 0.25$ $k_1 = 0.018$ $c_p = 1.15$ for 0 to 10 m,
$a_y(425) = 0.20$ $k_1 = 0.020$ $c_p = 0.92$ for 10 to 20 m,
$a_y(425) = 0.15$ $k_1 = 22$ $c_p = 71$ for 20 to 40 m,
$a_y(425) = 0.11$ $k_1 = 27$ $c_p = 60$ for 40 to 70 m.

The spectra are shown in Fig 8. For comparison, the same drawing gives examples of $c(\lambda)$ spectra for the Baltic, selected as extrema from the paper [8]. The main property of the spectra found for the studied environment is a distinctly weaker increase in c towards short waves, as compared with the Baltic spectra, and an analogous displacement of the minimum towards short waves occurring in the wave band of about 550 nm in the surface layer and about 525 nm at the bottom.

The flat form of the spectra and the small values of the coefficients of absorption in yellow substance, a_y (425 nm), indicate that the concentration of yellow substance is very small and decreases distinctly with depth, as compared with the Baltic, for which a_y (425 nm) $\simeq 0.4$ m^{-1}, as found for the spectra shown in Fig. 8. It should be mentioned that values determined for the Ezcurra Inlet are most probably overestimated, because of the possible increase in the coefficient of attenuation in suspended matter, with decreasing wavelength, as opposed to the Baltic spectra. Since the coefficient of absorption in organic yellow substance is small, it should be assumed that it is inorganic suspended matter that is responsible for attenuation of light in the studied environment.

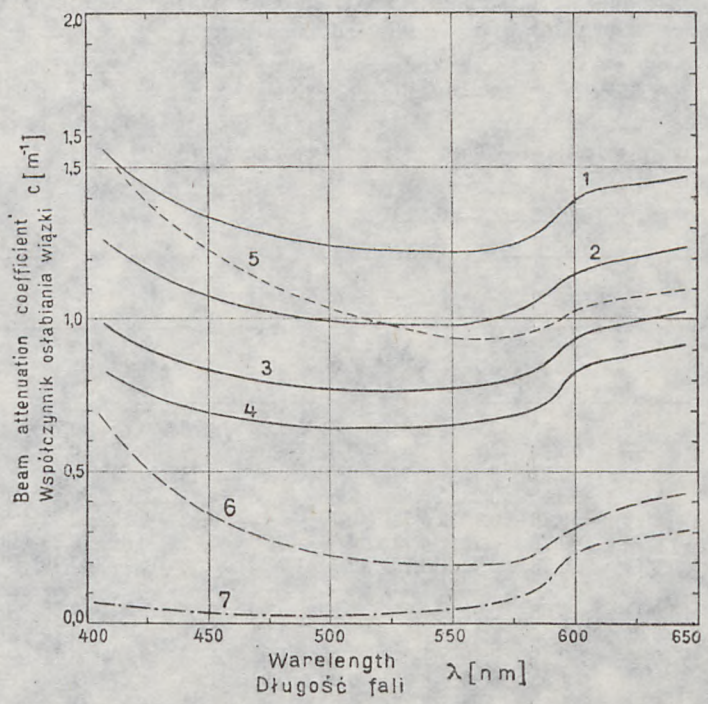

Fig. 8. Spectra of the beam attenuation coefficient at selected depth intervals, averaged over the whole period of measurements: *1* — 0—10 m, *2* — 10—20 m; *3* — 20—40 m; *4* — 40—70 m; *5*, *6* — the Baltic according to [8]; *7* — distilled water according to [4]

Rys. 8. Uśrednione w całym okresie pomiarów widma współczynnika osłabiania wiązki promieni w wybranych przedziałach głębokości: *1* — 0—10 m; *2* — 10—20 m; *3* — 20—40 m; *4* — 40—70 m;*5*, *6* — Bałtyk wg [8], *7* — woda destylowana wg [4]

3. ATTENUATION OF NATURAL LIGHT

The coefficient of diffusive attenuation of downward irradiance averaged through the euphotic zone [6] has been taken as the parameter that characterizes the attenuation of natural light. The coefficient was computed from the measured data of vertical changes in the downward irradiance:

$$k_d = \frac{\log 100}{z_{1\%}} \tag{5}$$

in which $z_{1\%}$ is the boundary of the euphotic zone to which 1 per cent of the surface light is incident.

The measurements were conducted in three wavelengths, taken si-

Table 1. Beam attenuation coefficient, c (525 nm), at various depths covering the range of 1—70 m, and downward irradiance attenuation coefficient, $\overline{k_d}$ (525 nm), averaged over the depth range from 0 to about 30 m, Ezcurra Inlet, 20 December 1977 — 10 March 1978

Tab. 1. Współczynnik osłabiania wiązki promieni c (525 nm) na różnych głębokościach w przedziale 1—70 m i średni współczynnik dyfuzyjnego osłabiania oświetlenia $\overline{k_d}$ (525 nm) uśredniany w przedziale głębokości 0—ok. 30 m. Fiord Ezcurra, 20.12.1977—10.03.1978

f (525 nm)	$\overline{k_d}$[m^{-1}]	c[m^{-1}]									
z [m] GMT	0—30	1	5	10	15	20	30	40	50	60	70
12.20.15	0,19	0,75	0,78	0,80	0,81	0,80	0,78	0,75	0,74	0,67	0,70
18	—	0,84	0,82	0,80	0,81	0,82	0,79	0,77	0,67	0,62	0,55
21	0,23	0,81	0,79	0,77	0,78	0,80	0,74	0,65	0,62	0,68	0,71
24	—	0,85	0,83	0,82	0,83	0,83	0,71	0,61	0,59	0,55	0,68
12.21.09	0,20	0,78	0,75	0,74	0,71	0,72	0,72	0,75	0,75	0,66	0,69
12	—	0,70	0,72	0,73	0,74	0,76	0,77	0,81	0,83	0,69	0,72
15	0,18	0,73	0,72	0,70	0,74	0,78	0,78	0,77	0,79	0,63	0,71
12.28.17	0,20	—	—	—	—	—	—	—	—	—	—
12.29.12	0,17	0,88	0,92	0,97	0,99	0,95	0,59	0,54	0,56	0,59	0,59
19	0,20	1,34	1,34	1,34	1,12	0,93	0,84	0,72	0,76	0,76	0,79
12.30.12	0,18	0,95	0,99	1,01	1,02	1,03	1,00	0,98	0,71	0,72	0,78
01.02.15	0,16	1,03	0,94	0,95	0,97	0,93	1,26	1,27	1,23	1,23	1,22
20	0,25	1,89	2,05	2,22	2,08	1,99	1,63	1,41	1,28	1,05	0,84
24	—	1,52	1,51	1,49	1,50	—	—	—	—	—	—
01.03.18	0,25	2,03	2,09	2,11	2,01	1,55	1,00	0,92	0,92	0,79	0,70
24	—	2,11	2,11	1,69	1,19	1,11	0,96	0,92	0,92	0,92	0,89
01.04.15	—	2,15	1,80	1,46	1,50	1,27	0,98	1,00	1,05	0,97	—
20	0,24	1,74	2,33	1,85	1,41	1,35	1,26	1,09	1,04	0,97	0,93
01.05.15	0,21	1,94	1,62	1,42	1,23	1,17	1,05	0,94	0,92	0,92	0,70
20	—	4,37	1,69	1,75	1,54	—	—	—	—	—	—
01.06.16	0,17	1,23	1,21	1,23	1,07	—	—	—	—	—	—
01.14.21	0,16	0,68	0,68	0,68	0,76	0,80	0,81	0,79	0,83	0,68	0,52
01.15.16	0,15	0,72	0,68	0,58	0,66	0,52	0,52	0,46	0,47	0,47	0,53
01.17.11	—	0,94	1,17	1,02	1,01	0,91	0,83	0,70	0,76	1,06	0,85
12	—	1,11	1,18	1,15	0,96	0,83	0,71	0,73	1,05	1,05	0,92
13	—	0,93	1,26	1,20	0,88	0,85	0,72	0,76	1,08	1,06	0,94
14	—	0,97	1,15	1,00	0,79	0,78	0,70	0,78	0,97	1,12	0,91
15	—	0,92	1,11	0,85	0,81	0,77	0,69	0,78	0,91	1,14	0,92
16	—	0,94	1,34	1,02	0,81	0,76	0,70	—	—	—	—
17	—	0,79	1,37	1,27	0,83	0,57	0,66	0,75	0,94	0,87	0,64
19	—	1,23	1,38	0,78	0,66	0,63	0,73	0,82	0,91	0,68	0,54
20	—	1,18	1,30	0,84	0,68	0,66	0,69	0,92	0,81	0,63	0,44
21	—	1,50	1,22	0,76	0,68	0,64	0,69	0,96	0,84	0,58	0,53
22	—	1,46	1,28	1,08	0,67	0,66	0,68	1,00	0,83	0,64	0,51
23	—	1,52	1,22	0.91	0,73	0,62	0,65	0,97	0,85	0,62	0,55
24	—	1,96	1,22	0,79	0,64	0,61	0,72	0,94	0,85	0,54	0,50
01.18.01	—	1,61	1,46	0,87	0,63	0,56	0,65	0,87	0,73	0,64	0,72
02	—	1,48	1,02	0,66	0,51	0,49	0,51	0,76	0,83	0,83	0,66
03	—	1,09	1,08	0,88	0,69	0,52	0,54	0,82	0,96	0,93	0,90
04	—	1,38	1,11	0,92	0,57	0,47	0,47	0,64	0,81	0,92	0,92
05	—	1,50	1,36	0,91	0,67	0,64	0,57	0,55	0,65	0,85	0,90
06	—	1,20	1,20	1,18	1,00	0,71	0,72	0,61	0,64	0,81	1,02
07	—	1,15	1,20	1,11	0,84	0,91	0,69	0,63	0,64	0,72	0,86
08	—	1,12	1,12	1,09	0,94	0,84	0,72	0,64	0,63	0,66	0,84

Table 1., cont.
Tab. 1., cd.

f(525 nm)	$\bar{k}_d$[m^{-1}]	c [m^{-1}]									
z [m] GMT	0—30	1	5	10	15	20	30	40	50	60	70
09	—	1,11	1,06	1,05	0,85	0,64	0,62	0,64	0,61	0,64	0,79
10	—	1,08	1,14	1,12	1,01	0,74	0,70	0,62	0,61	0,68	0,78
11	—	1,08	1,06	1,00	1,04	0,69	0,60	0,58	0,58	0,69	0,76
01.18.19	0,15	1,07	0,89	0,73	0,56	0,55	0,57	0,65	0,54	0,36	0,41
01.19.13	0,17	1,07	1,20	1,00	0,82	0,76	0,64	0,68	0,72	0,76	0,82
01.21.14	0,17	1,15	1,17	1,14	1,06	1,09	0,87	0,68	0,72	0,72	0,78
21	0,21	1,99	1,86	1,59	0,66	0,56	0,47	0,32	0,23	0,23	0,23
01.24.16	0,16	0,87	0,90	0,83	0,71	0,70	0,65	0,49	0,51	0,53	0,59
22	0,16	0,80	0,81	0,76	0,49	0,46	0,37	0,30	0,28	0,21	0,30
01,26,03	—	1,25	0,88	1,02	0,72	0,32	0,19	0,20	0,15	0,18	0,24
01.27.12	0,13	0,92	0,94	0,97	0,70	0,70	0,52	0,55	0,40	0,40	0,44
17	0,13	0,86	0,87	0,85	0,87	0,57	0,45	0,40	0,33	0,37	0,40
01.29.03	—	1,00	0,36	0,28	0,28	0,25	0,13	0,13	0,17	0,19	0,34
01.30.12	—	0,86	0,88	0,48	0,42	0,36	0,30	0,23	0,23	0,24	—
19	—	0,79	0,77	0,71	0,68	0,60	0,49	0,39	0,27	0,36	0,43
02.01.12	0,29	1,59	1,87	1,92	2,00	1,93	1,15	0,49	0,44	0,42	—
02.03.11	—	1,22	1,07	0,82	0,70	0,59	0,37	0,42	0,48	0,51	0,54
02.06.20	0,17	1,02	1,03	0,98	0,92	0,89	1,09	0,82	0,69	0,67	0,69
02.07.17	0,23	1,83	1,83	1,80	1,64	0,97	0,83	0,81	0,70	0,66	0,75
02.08.11	—	1,23	1,23	1,21	1,18	1,14	0,87	0,47	0,49	0,46	0,48
02.10.12	0,20	1,48	1,49	1,27	1,06	0,98	0,86	0,84	0,73	0,80	—
02.11.12	0,20	1,19	1,32	1,21	1,21	1,06	0,95	0,83	0,83	0,89	0,90
02.14.12	0,17	0,97	0,98	0,82	0,81	0,83	0,85	0,87	0,82	0,77	—
19	0,24	1,32	1,23	1,23	1,05	0,89	0,75	0,72	0,76	0,82	0,83
02.16.19	0,23	1,34	1,34	1,31	1,28	1,28	0,93	0,78	0,77	0,54	0,43
02.21.15	0,18	0,93	0,94	0,89	0,87	0,87	0,85	0,78	0,53	0,54	0,61
22	0,19	0,99	1,00	0,97	0,81	0,69	0,45	0,47	0,27	0,27	0,30
02.24.12	0,20	—	—	—	—	—	—	—	—	—	—
15	—	2,76	1,69	0,87	0,89	0,70	0,60	0,49	0,52	0,51	—
18	0,20	1,69	1,53	0,96	0,78	0,68	0,63	0,59	0,57	0,54	0,97
21	—	2,53	0,97	0,71	0,54	0,53	0,34	0,33	0,33	0,33	0,40
24	—	2,38	2,40	1,29	1,15	0,55	0,33	0,35	0,34	0,37	0,43
02.25.03	—	1,83	1,54	0,91	0,74	0,63	0,46	0,37	0,41	0,41	—
06	—	1,93	1,00	0,83	0,70	0,66	0,42	0,37	0,40	0,27	—
09	—	1,98	1,95	1,02	0,61	0,61	0,65	0,45	0,37	0,38	0,39
12	0,21	1,17	1,19	0,95	0,72	0,58	0,51	0,47	0,39	0,36	0,40
02.28.12	0,18	0,81	0,83	0,85	0,82	0,78	0,81	0,81	0,80	0,83	0,98
03.03.14	0,20	2,00	0,97	0,87	0,87	0,87	0,64	0,48	0,30	0,25	—
03.04.12	0,16	1,03	0,87	0,69	0,58	0,56	0,56	0,36	0,26	0,24	0,29
16	0,19	1,23	1,28	1,30	1,16	0,76	0,46	0,28	0,13	0,17	0,23
03.07.12	0,25	1,38	1,42	1,45	1,13	1,11	0,99	0,93	0,86	0,95	0,74
16	0,24	1,93	1,64	1,17	1,15	1,15	1,00	0,95	0,56	0,43	0,61
03.10.12	0,23	1,83	1,83	1,80	1,74	1,54	1,13	1,17	1,21	1,22	1,23
16	0,27	1,94	1,93	1,96	1,89	1,89	1,39	1,31	1,23	1,20	1,16

milarly as in the case of the beam attenuation, viz. $\lambda=425$, 525 and 600 nm. The irradiance for the couples $\lambda=425$ and $\lambda=525$, or 600 and 525 nm, was measured simultaneously. The wavelength $\lambda=525$ nm, was taken as a reference, and the boundary of the euphotic zone was com-

Table 2. Beam attenuation coefficient, c (425 nm), at various depths covering the range of 1—70 m, and downward irradiance attenuation coefficient, $\overline{k_d}$ (425 nm), averaged over the depth range from 0 to about 20 m. Ezcurra Inlet, 20 December 1977 — 4 February 1978.

Tab. 2. Współczynnik osłabiania wiązki promieni c (425 nm) na różnych głębokościach w przedziale 1—70 m i średni współczynnik dyfuzyjnego osłabiania oświetlenia $\overline{k_d}$ (425 nm) uśredniany w przedziale głębokości 0—ok. 20 m. Fiord Ezcurra, 20.12.1977—04.02.1978.

f(425 nm)	$\overline{k_d}$[m^{-1}]	c [m^{-1}]									
z [m] GMT	0—20	1	5	10	15	20	30	40	50	60	70
12.20.15	0,24	0,95	0,95	0,94	0,96	0,95	0,92	0,85	0,73	0,63	0,65
18	—	0,98	1,02	1,00	0,99	0,99	0,86	0,85	0,78	0,67	0,66
21	0,25	0,93	0,93	0,94	0,92	0,92	0,74	0,68	0,56	0,64	0,67
12.21.09	0,25	0,89	0,89	0,87	0,79	0,78	0,78	0,73	0,71	0,62	0,59
12	—	0,75	0,78	0,78	0,78	0,82	0,85	0,81	0,73	0,69	0,70
15	0,23	0,85	0,84	0,85	0,87	0,87	0,85	0,81	0,65	0,59	0,61
12.26.15	—	1,35	1,27	1,10	1,05	0,95	0,80	0,66	0,50	0,48	0,45
21	—	1,69	0,95	0,74	0,66	0,63	0,61	0,53	0,41	0,30	0,32
12.27.15	—	1,90	1,92	1,81	1,24	1,07	0,91	0,81	0,64	0,45	—
20	—	1,46	1,37	1,29	1,14	0,79	0,61	0,56	0,55	0,56	0,41
12.28.11	—	1,91	1,72	1,10	1,08	0,92	0,68	0,65	0,52	0,43	—
17	0,30	1,83	1,75	1,36	1,12	1,00	0,87	0,76	0,69	0,50	0,50
12.29.12	0,23	1,06	1,08	1,12	1,07	0,89	0,59	0,53	0,52	0,50	0,46
19	0,26	1,56	1,55	1,61	1,44	1,43	1,05	0,87	0,78	0,81	0,80
12.30.12	0,23	1,16	1,18	1,22	1,22	1,22	1,19	1,18	0,80	0,75	0,76
19	—	1,14	1,14	1,10	1,12	1,14	1,12	0,93	0,87	—	—
01.01.23	—	0,99	0,97	0,95	0,95	—	—	—	—	—	—
01.02.15	0,21	1,21	1,18	1,16	1,15	1,10	1,52	1,43	1,32	1,25	—
20	0,33	1,95	1,97	2,02	1,97	1,98	1,97	1,86	1,72	1,46	1,09
24	—	2,17	2,13	2,12	2,02	—	—	—	—	—	—
01.03.18	0,36	2,34	2,39	2,34	1,55	1,36	1,20	1,11	0,92	0,65	0,63
24	—	2,76	2,69	2,81	1,68	1,43	1,23	1,12	1,06	0,95	0,87
01.04.15	—	2,18	2,07	1,90	1,68	1,39	1,30	1,20	1,12	1,03	—
20	0,33	2,18	2,72	2,26	1,83	1,82	1,61	1,32	1,28	1,30	0,97
01.05.15	0,33	2,37	2,10	1,77	1,46	1,34	1,17	1,04	0,94	0,92	0,94
20	—	3,85	2,52	2,12	1,88	—	—	—	—	—	—
01.06.16	0,22	1,68	1,62	1,11	1,17	—	—	—	—	—	—
01.14.21	0,20	0,91	0,90	0,89	0,89	0,89	0,91	0,89	0,87	0,54	0,51
01.15.16	0,18	1,01	1,04	1,00	0,88	0,81	0,70	0,62	0,54	0,48	0,52
01.18.19	0,17	1,14	1,24	0,89	0,66	0,63	0,69	0,81	0,62	0,43	0,40
01.19.13	0,24	1,54	1,46	1,27	1,23	0,96	0,80	0,81	0,84	0,84	0,84
01.21.14	0,23	1,39	1,42	1,39	1,36	1,34	0,85	0,78	0,76	0,73	0,78
21	0,30	2,45	2,45	2,24	0,79	0,67	0,48	0,44	0,18	0,11	0,11
01.24.16	0,21	1,07	1,06	0,92	0,80	0,83	0,73	0,58	0,51	0,54	0,57
22	0,18	0,98	0,99	0,99	0,77	0,49	0,47	0,41	0,37	0,23	0,24
01.26.03	—	1,55	1,55	1,19	1,21	1,16	0,67	0,52	0,31	0,31	0,26
04	—	1,62	1,14	1,28	1,27	1,17	0,56	0,51	0,50	0,33	0,31
01.27.12	0,15	1,17	1,17	1,16	1,05	0,84	0,63	0,63	0,47	0,44	0,49
17	0,16	1,10	1,10	1,13	0,87	0,69	0,63	0,53	0,46	0,46	0,45
01.29.03	—	2,31	0,84	0,36	0,31	0,18	0,19	0,21	0,22	0,22	0,29
01.30.12	—	1,02	0,90	0,85	0,60	0,52	0,39	0,30	0,22	0,21	—
19	—	1,07	1,05	0,96	0,86	0,67	0,56	0,45	0,31	0,26	0,33
02.01.12	0,39	1,97	2,13	2,10	2,17	2,17	1,58	0,45	0,38	0,29	—
02.03.11	—	1,76	1,48	0,85	0,77	0,63	0,45	0,45	0,51	0,46	0,45

Table 2., cont.
Tab. 2., cd.

f(425 nm)	$\bar{k}_d$[m^{-1}]	c [m^{-1}]									
z [m] GMT	0—20	1	5	10	15	20	30	40	50	60	70
12	—	1,20	1,35	1,05	0,94	0,87	0,46	0,50	0,52	0,53	0,51
13	—	1,65	1,54	1,03	0,81	0,47	0,46	0,45	0,47	0,48	0,47
14	—	1,10	0,96	0,92	0,91	0,81	0,52	0,53	0,53	0,60	0,57
15	—	1,65	0,83	0,68	0,49	0,53	0,47	0,47	0,47	0,51	0,51
16	—	1,13	0,83	0,74	0,62	0,52	0,49	0,49	0,51	0,51	0,51
17	—	0,77	0,77	0,63	0,63	0,50	0,48	0,48	0,45	0,53	0,47
18	—	1,93	0,92	0,70	0,63	0,56	0,55	0,53	0,54	0,44	0,43
19	—	1,41	0,60	0,52	0,52	0,52	0,48	0,47	0,44	0,38	0,37
20	—	1,33	1,46	1,38	0,57	0,54	0,54	0,50	0,33	0,15	0,15
21	—	1,88	1,62	0,54	0,50	0,48	0,49	0,42	0,38	0,37	0,22
22	—	1,82	0,89	0,69	0,65	0,66	0,52	0,43	0,31	0,20	0,15
23	—	1,52	1,48	1,22	0,83	0,66	0,54	0,53	0,42	0,32	0,21
24	—	1,43	1,46	1,21	0,82	0,76	0,57	0,55	0,46	0,35	0,17
02.04.01	—	1,82	1,65	1,49	1,33	1,03	0,72	0,59	0,52	0,34	0,37
02	—	1,34	1,48	1,43	0,82	0,83	0,67	0,60	0,58	0,53	0,41
04	—	1,24	1,23	1,23	0,97	0,95	0,74	0,68	0,67	0,53	0,44
05	—	1,03	1,03	1,05	1,07	0,99	1,01	0,93	0,73	0,67	0,39
06	—	1,21	1,08	1,04	0,94	0,94	0,94	0,94	0,85	0,85	0,54
07	—	1,10	1,08	1,08	1,05	1,04	0,92	0,84	0,72	0,51	—
08	—	0,97	0,98	0,96	0,93	0,92	0,90	0,83	0,69	0,55	0,45
09	—	0,95	0,75	0,62	0,62	0,56	0,54	0,54	0,56	0,58	0,48
10	—	0,82	0,84	0,72	0,70	0,69	0,63	0,63	0,61	0,65	0,56
11	—	1,08	1,01	1,19	0,73	0,67	0,58	0,56	0,53	0,59	0,54

puted for this length, as the one that is closest to the maximum of transmission. The computed values of coefficients $\bar{k}_d$ for the selected wavelengths are given in Tables 1, 2 and 3.

The temporal variation of the coefficient of attenuation and the range of euphotic zone, averaged through ten-day periods, are presented in Fig. 9. The most characteristic property of the variation is observed as the pronounced extremum of the coefficient of attenuation and the range of euphotic zone in the third and fourth decade of investigations. Since the measurements were carried out only once, it is difficult to judge how typical this extremum could be for a longer period of observations covering several years.

Further averaging of the series over two 40-day period marked with a broken line, indicates an increase in the resulting coefficient of irradiance attenuation in the second half of the measurements, similarly to the changes in the c-coefficient in the surface layer.

The next two drawings present distributions of relative frequencies of occurrence of k_d, at intervals of 0.04 m^{-1} (Fig. 10) and the range of euphotic zone $z_{1\%}$ at intervals of 4 m (Fig. 11). As for the beam attenu-

Table 3. Beam attenuation coefficient, c (600 nm), at various depths covering the range of 1—70 m, and downward irradiance attenuation coefficient, k_d (600 nm), averaged over the depth range from 0 to about 20 m. Ezcurra Inlet, 6 February 1978 — 10 March 1978.

Tab. 3. Współczynnik osłabiania wiązki promieni c (600 nm) na różnych głębokościach w przedziale 1—70 m oraz średni współczynnik dyfuzyjnego osłabiania oświetlenia $\overline{k_d}$ (600 nm) uśredniany w przedziale głębokości 0— ok. 20 m. Fiord Ezcurra, 6.02.1978—10.03.1978.

f (600 nm)	$\overline{k_d}$[m^{-1}]	c [m^{-1}]									
z [m] GMT	0—20		5	10	15	20	30	40	50	60	70
02.06.20	0,33	0,92	0,93	0,92	0,87	0,79	1,00	0,93	0,61	0,59	0,58
02.07.17	0,34	1,69	1,69	1,64	1,42	0,85	0,85	0,81	0,75	0,66	0,72
02.08.22	—	1,39	1,38	1,38	1,34	1,29	0,85	0,64	0,63	0,61	0,56
02.10.12	0,35	1,45	1,43	1,21	1,08	0,91	0,85	0,85	0,77	0,88	—
02.11.12	0,32	1,48	1,23	1,04	1,00	0,97	0,83	0,75	0,78	0,79	0,83
02.14.12	0,31	1,34	1,26	1,01	0,99	1,02	1,00	1,03	1,01	0,77	—
19	0,33	1,44	1,43	1,15	0,95	0,87	0,89	0,87	0,92	0,95	0,99
02.16.19	0,34	1,54	1,51	1,46	1,34	1,26	1,13	0,95	0,94	0,63	0,61
02.17.11	—	1,64	1,64	1,67	1,66	1,50	1,10	0,79	0,76	0,81	0,81
12	—	1,60	1,58	1,57	1,49	1,40	1,38	0,91	0,83	0,67	0,47
13	—	1,50	1,50	1,35	1,18	1,24	0,96	0,76	0,58	0,46	0,43
14	—	1,40	1,44	1,45	1,03	0,84	0,85	0,65	0,48	0,42	0,43
15	—	1,41	1,46	1,44	1,36	1,12	0,79	0,49	0,40	0,38	0,39
16	—	1,50	1,48	1,39	1,32	1,04	0,72	0,53	0,42	0,41	0,38
17	—	1,59	1,58	1,57	1,53	1,49	0,83	0,70	0,45	0,44	0,41
18	—	1,51	1,54	1,55	1,43	1,39	1,01	0,70	0,60	0,48	0,45
20	—	1,72	1,57	1,64	1,62	1,43	1,14	0,88	0,66	0,61	0,50
21	—	1,56	1,56	1,55	1,49	1,35	1,15	0,82	0,67	0,63	0,48
22	—	1,52	1,50	1,37	1,27	1,27	0,96	0,69	0,61	0,59	0,54
23	—	1,50	1,54	1,50	1,41	1,42	0,99	0,71	0,58	0,63	0,61
24	—	1,49	1,49	1,47	1,47	1,49	1,45	1,14	0,82	0,64	0,59
02.18.01	—	1,41	1,38	1,38	1,38	1,38	1,36	1,39	1,28	0,66	—
02	—	1,33	1,36	1,34	1,36	1,36	1,36	1,39	1,17	0,74	0,73
03	—	1,38	1,38	1,40	1,42	1,41	1,46	1,47	1,47	1,38	1,22
04	—	1,38	1,38	1,38	1,42	1,46	1,48	1,43	1,44	1,39	0,70
05	—	1,34	1,37	1,40	1,40	1,40	1,50	1,54	1,69	1,58	1,46
08	—	1,27	1,27	1,27	1,26	1,30	1,32	1,29	1,27	1,29	1,30
09	—	1,42	1,44	1,50	1,38	1,36	1,20	1,42	1,00	0,93	1,46
10	—	1,41	1,40	1,42	1,37	1,19	0,97	0,90	0,87	1,14	1,19
11	—	1,67	1,67	1,67	1,59	1,51	1,40	0,90	0,81	0,84	0,90
02.21.15	0,31	1,10	1,07	1,05	1,07	1,05	0,84	0,74	0,68	0,72	0,74
22	0,31	1,17	1,11	1,08	0,93	0,86	0,67	0,68	0,60	0,51	0,48
02.24.12	0.34	1,11	1,06	1,05	1,05	1,04	0,85	0,76	0,82	0,70	0,72
18	0,32	2,56	1,40	1,14	0,87	0,79	0,71	0,67	0,68	0,68	0,68
24	—	2,44	2,32	1,34	0,95	0,73	0,54	0,57	0,57	0,57	0,58
02.25.06	—	2,36	2,28	2,10	0,96	0,76	0,73	0,65	0,62	0,65	0,58
12	0,32	1,40	1,43	1,30	1,14	1,06	0,77	0,76	0,73	0,72	0,68
02.28.12	0,31	1,01	1,00	1,01	0,96	0,92	0,96	0,92	0,94	0,98	1,08
03.03.14	0,30	2,24	2,24	1,20	1,10	1,03	0,82	0,81	0,58	0,57	0,70
03.04.12	0,31	1,34	1,34	1,22	1,05	0,79	0,79	0,74	0,59	0,49	0,48
16	0,31	1,45	1,46	1,46	1,27	1,15	0,72	0,58	0,40	0,40	0,44
03.07.12	0,39	1,68	1,65	1,67	1,58	1,27	1,18	1,23	1,32	1,15	1,05
16	0,35	2,33	2,33	1,19	1,24	1,21	1,14	1,22	0,97	0,74	0,86
03.10.12	0,36	2,13	2,13	2,14	2,06	2,00	1,55	1,38	1,38	1,39	1,38
16	0,38	2,06	2,10	2,15	2,15	1,93	1,64	1,52	1,46	1,53	1,49

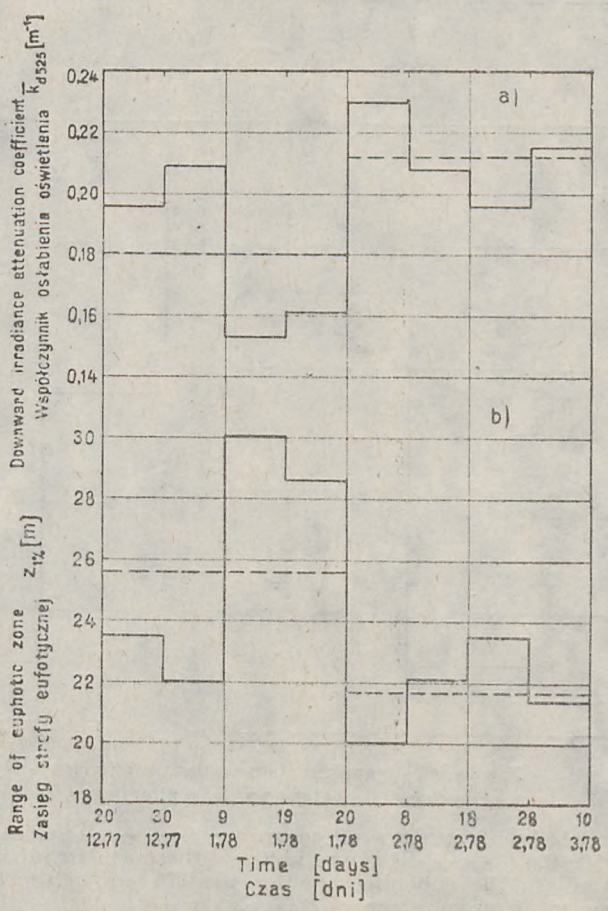

Fig. 9. Time function of the values of mean irradiance diffusive attenuation coefficient for the euphotic zone (a), and the range of the euphotic zone (b), both averaged over 10-day (————), and 40-day (- - - - - - -) periods for the 525 nm light wavelength

Rys. 9. Przebieg czasowy uśrednianych w odcinkach 10-dniowych (————) i 40-dniowych (- - - - - - -) wartości średniego dla strefy eufotycznej współczynnika dyfuzyjnego osłabiania oświetlenia (a) i zasięgu strefy eufotycznej (b) dla długości fali świetlnej 525 nm

ation coefficient, these distributions can be approximated by the gamma function for probability density, with the following parameters:

— mean value $\bar{k}_d = 0.197$ m^{-1} and variance $\delta^2_k = 0.0013$ for the coefficient of irradiance attenuation

— mean value $z_{1\%} = 24.2$ m and variance $\delta^2_z = 19.8$ for the range of the auphotic zone.

In both cases, the relative standard deviation is 18.4% which indicates a relatively small scatter around the mean value, comparable with

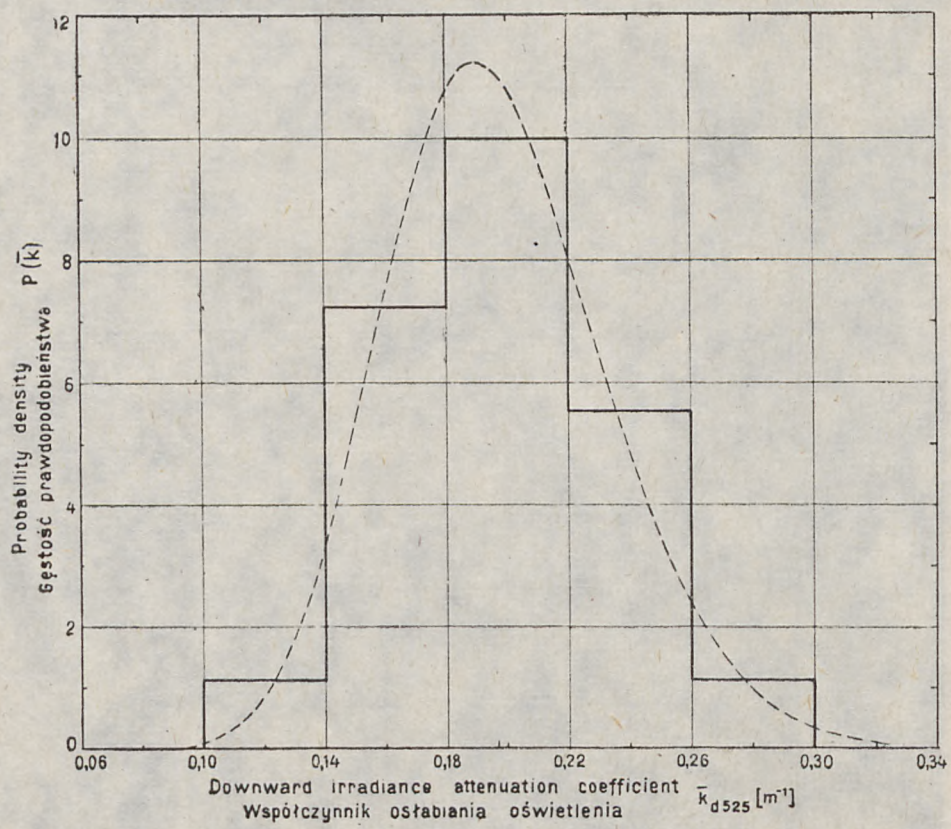

Fig. 10. Relative frequency of occurence (————) and the distribution of probability density (- - - - - - -) of the value of the mean irradiance diffusive attenuation coefficient in the euphotic zone for the 525 nm light wavelength found for the whole period of measurements

Rys. 10. Znaleziona dla całego okresu pomiarów względna częstość występowania (————) i rozkład gęstości prawdopodobieństwa (- - - - - -) wartości średniego dla strefy eufotycznej współczynnika dyfuzyjnego osłabiania oświetlenia dla długości fali świetlnej 525 nm

the scatter of the coefficient of beam attenuation in the surface layer. Compared with the latter, the values $\bar{k}_d$ and $z_{1\%}$ are much more symmetric, so that the mean values are closer to the most probable values.

A certain similarity of the distributions of the coefficients of beam attenuation and irradiance attenuation suggest that the values $\bar{k}_d$ and $\bar{c}$, the latter averaged within the euphotic zone, can be correlated. Fig. 12 presents the data obtained from almost simultaneous measurements of the above coefficients: mean irradiance attenuation in the euphotic zone and beam attenuation, averaged at the some depth interval. The regression equation for both sets reads:

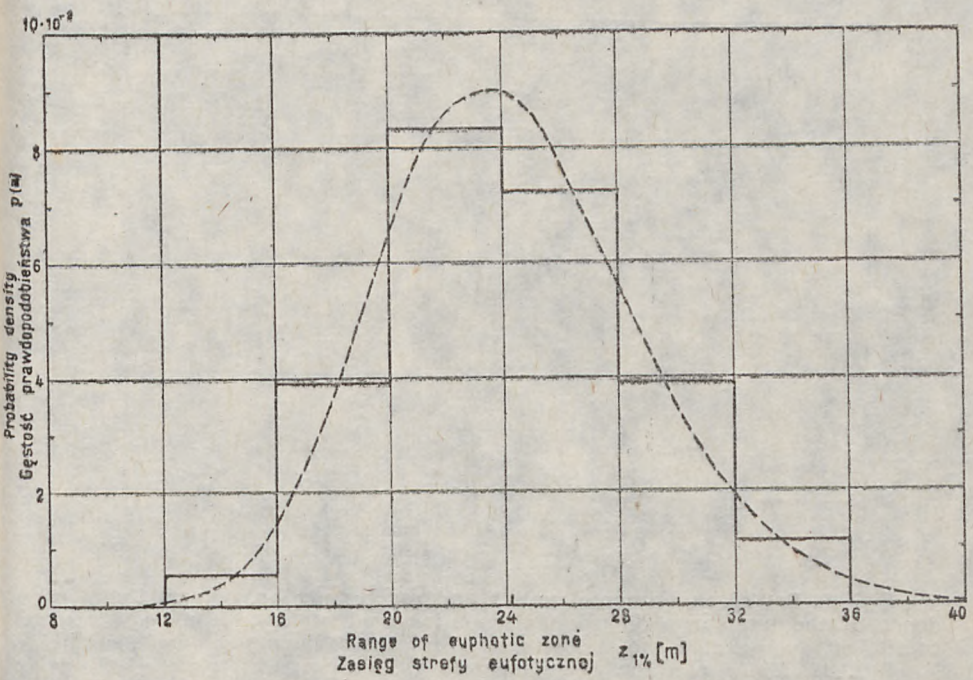

Fig. 11. Relative frequency of occurence (————) and distribution of probability density (- - - - - -) of the range of the euphotic zone, found for the whole period of measurements

Rys. 11. Znaleziona dla całego okresu pomiarów względna częstość występowania (————) i rozkład gęstości prawdopodobieństwa (- - - - - -) zasięgu strefy eufotycznej

$$\bar{k}_{d525} = (0.076 \pm 0.008)\ \bar{c}_{525} + (0.113 \pm 0.009) \qquad (6)$$

with the coefficient of correlation $\varrho \simeq 0.84$.

Since the amount of data is rather small, and as the measurements were carried out at different places and times, the correlation shown seems to be fairly good. It can be used to supplement the data for irradiance attenuation based on results for the coefficient of beam attenuation, more ample than k_d data.

As mentioned, the basic measurements of k_d were conducted in the wavelength of 525 nm. However, k_d was always measured additionally for 425 or 600 nm as a supplement to the more accurate [13] spectral characteristics carried out in seven bands by Woźniak and Hapter. The spectral measurements in seven channels usually yielded values of k_d averaged for diurnal periods, mostly, however for a part of the euphotic zone (5 to 20 m), which can cause a certain divergence in results, particularly because of quite considerable horizontal stratification of optical properties. The correlations of the coefficients in the euphotic zone, mea-

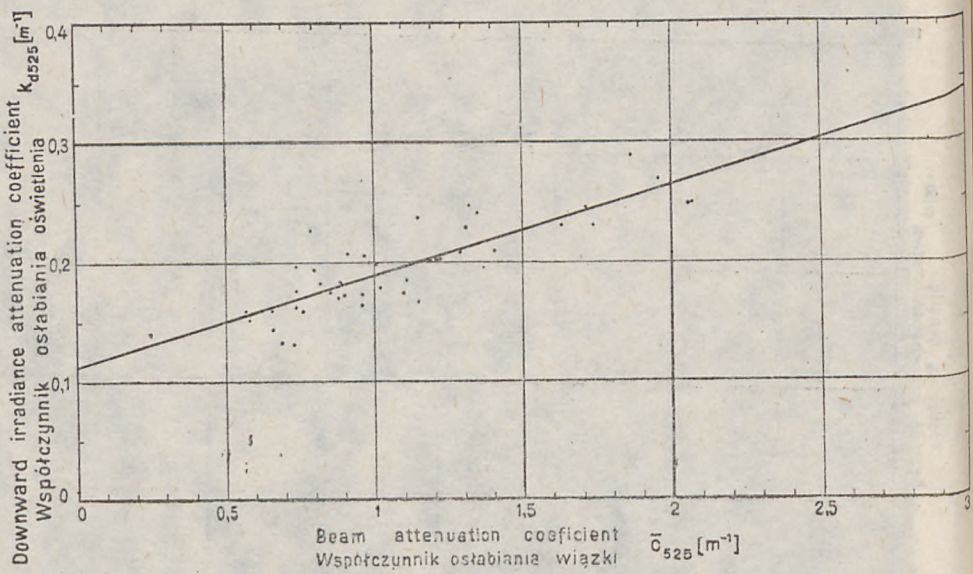

Fig. 12. Set of experimental points and regression line, determining the dependence of the irradiance diffusive attenuation coefficient on the beam attenuation coefficient averaged in the euphotic zone, for the 525 nm light wavelength

Rys. 12. Zbiór punktów pomiarowych i linia regresji określające zależność współczynnika dyfuzyjnego osłabiania oświetlenia od uśrednionego w strefie eufotycznej współczynnika osłabiania wiązki promieni, dla długości fali świetlnej 525 nm

sured in the three wavelengths, are given in. Fig. 13, with the following equations of regression:

$$\bar{k}_{d425} = (1.580 \pm 0.085)\, \bar{k}_{d525} - (0.051 \pm 0.016)$$

with the coefficient of correlation $\varrho \simeq 0.97$, (7)

$$\bar{k}_{d600} = (0.732 \pm 0.121)\, \bar{k}_{d525} + (0.180 \pm 0.025)$$

with the coefficient of correlation $\varrho \simeq 0.82$.

One should regard these relationships with caution, because of the small amount of data, both for the above equations and for statistical distributions of k_{d525}. Nevertheless, some conclusions can be drawn, e.g. as to the optical type of the studied environment. By comparing the mean values of k_d (in the wavelengths mentioned $\bar{k}_{d425} = 0.26$, $\bar{k}_{d525} = 0.20$ and $\bar{k}_{d600} = 0.33$) with the values for the waters classified by Jerlov [6] one can ascertain that the investigated waters do not fall into any of the accepted categories. While type 3 (including the Baltic) describes well the data for 525 and 600 nm, the results for 425 nm are distinctly more „clear", indicating category between types III and I. This similar to the spectral results for the coefficient of beam attenuation suggests a minor contribution of the absorption in organic yellow substance in the total attenuation of light.

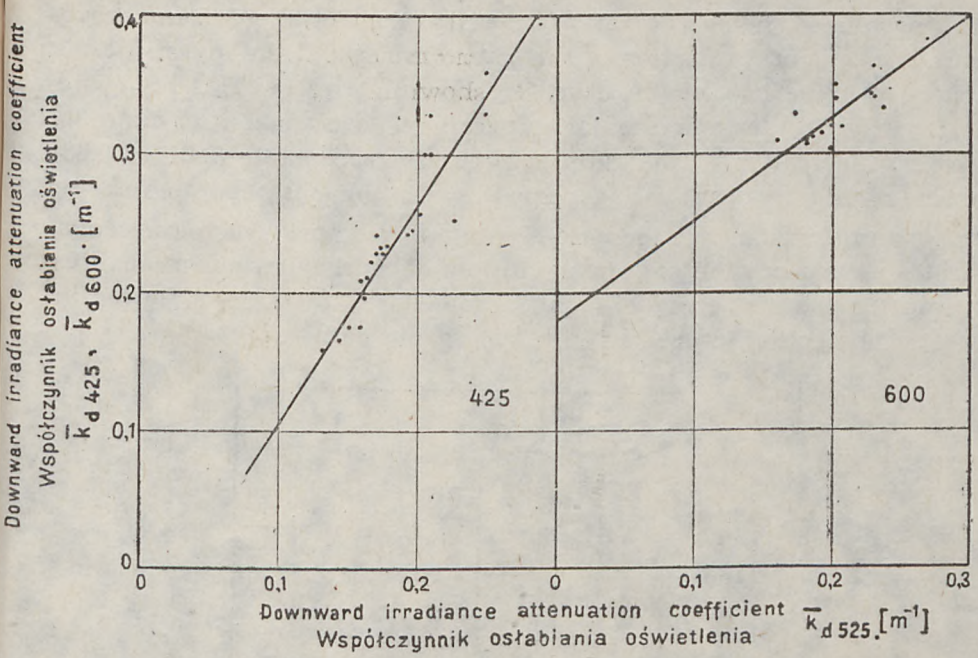

Fig. 13. Set of experimental points and regression lines, determining the dependence of the irradiance diffusive attenuation coefficientc for the 424 and 600 nm light wavelengths on the coefficient for 525 nm

Rys. 13. Zbiór punktów pomiarowych i linie regresji określające zależność współczynników dyfuzyjnego osłabiania oświetlenia dla długości fali świetlnej 425 i 600 nm współczynnika dla 525 nm

4. SCATTERING AND ABSORPTION OF LIGHT

Basing on the results for the coefficients of irradiance attenuation and beam attenuation, presented in the preceding chapter one can estimate the contribution of scattering and absorption to the process of light attenuation. Let us employ the well-known relationship between the coefficient of irradiance attenuation, k, and the coefficient of light absorption, a, derived from the law of energy conservation [3, 10]:

$$a = \overline{k\cos\vartheta} \tag{8}$$

in which $\overline{\cos\vartheta}$ is the ratio of irradiance to scalar irradiance.

Assuming that the downward irradiance is much higher than the upward and taking $\overline{\cos\vartheta} = 0.85$ [5] one obtains the following formula

$$a \simeq 0.85\, k_d \tag{9}$$

The correlation between $\bar{k}_d$ and $\bar{c}$, shown previously, enables the determination of ω_o, a parameter widely used in marine optics, the so-called

scattering albedo, being the ratio $\bar{b}/\bar{c}=1-\bar{a}/\bar{c}$. For the 525-nm wavelength, the temporal variation of this ratio throughout the investigations, averaged over periods of ten days, is shown in Fig. 14. This high irregularity may be due to accumulating errors of measurement of c and k_d. However, the scatter of the ratio is generally acceptable (0.81 to 0.88). Further averaging over 40-day periods, with the observed increase of $\omega_o=\bar{b}/\bar{c}$ and simultaneous increase of $\bar{c}$ and $\bar{k}_d$ (see previous paragraphs), indicates a clear-cut increase in the inflow of inorganic suspensions, responsible for the scattering of light, accompanied by a much lower increase in absorption, caused mainly by organic matter.

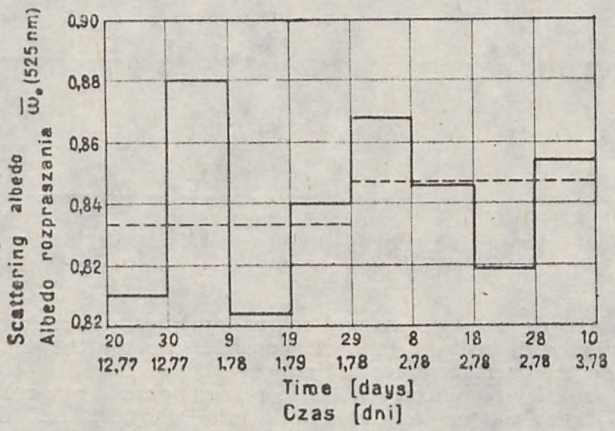

Fig. 14. Time function of the scattering albedo values averaged over 10-day (————) and 40-day (- - - - - - -) time intervals, for the 525 nm light wavelength
Rys. 14. Przebieg czasowy uśrednianych w odcinkach 10-dniowych (————) i 40-dniowych (- - - - - - -) wartości albeda rozpraszania, dla długości fali świetlnej 525 nm

Irrespective of the period of averaging, the mean value of b/c remains very high. Since this depends very little on light wavelength, the previous conclusions about prevailing nonselective scattering in suspensions, in the process of light attenuation, are substantiated.

Minor selectivity and the high ratios of b/c, as related to other environments, are to a certain extent illustrated by the figures given below for the Ezcurra Inlet, the Baltic and the Gulf of Gdańsk [12]:

Ezcurra Inlet	$b/c_{425}=0.83$	$b/c_{525}=0.85$	$b/c_{600}=0.78$
Baltic	0.4	0.8	0.6
Gulf of Gdańsk	0.4	0.6	0.4

In order to supplement the characteristics of the albedo of scattering in the waters investigated, Fig. 15 presents the possible variation of b/c

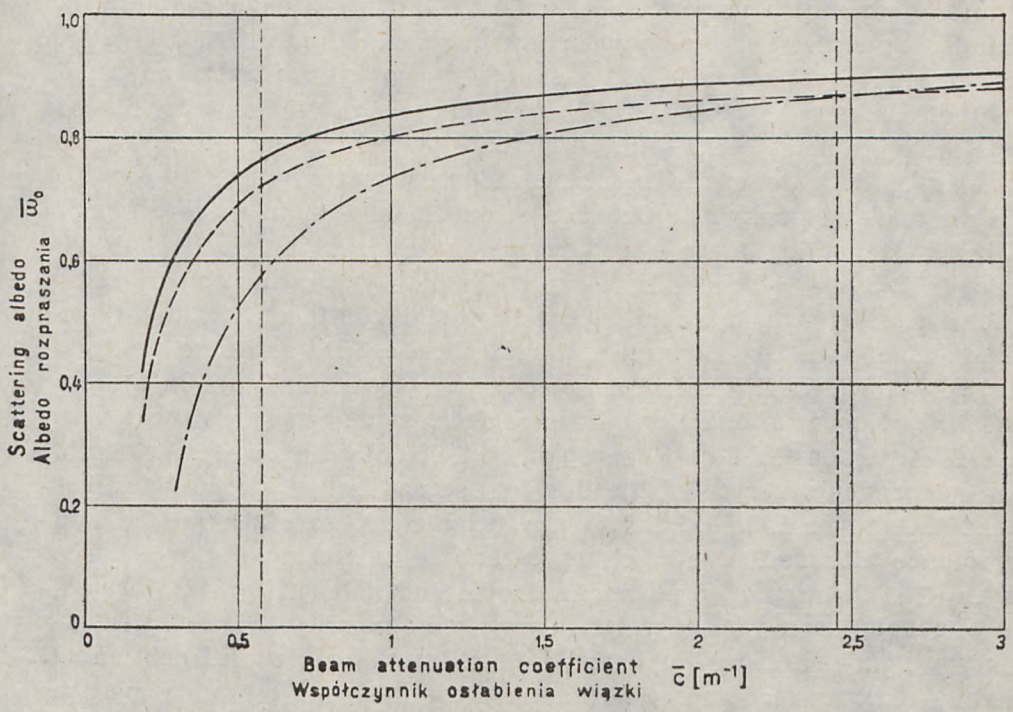

Fig. 15. Dependence of the scattering albedo on the value of the beam attenuation coefficient for light wavelengths of 425 nm (- - - - - - -), 525 nm (————) and 600 nm (— • —)

Rrys. 15. Zależność albeda rozpraszania od wartości współczynnika osłabiania wiązki promieni dla długości fali świetlnej 425 nm (- - - - - - -), 525 nm (————) i 600 nm (— • —)

versus the coefficient of attenuation, for these wavelengths. The drawing its based on the linear correlations presented above. The vertical broken lines give approximate boundaries (upper for 425 nm and lower for 525 nm) of the range of variability of the coefficient c averaged on the euphotic zone. Within the limits indicated, the greatest albedo of scattering always corresponds to 525 nm, while the lowest value marks the 600-nm wavelength. Decrease in the coefficient of attenuation is accompanied by a decrease in b/c, fairly modest in the short as well medium waves (425 and 525 nm), and much steeper in the red (600 nm).

5. SUMMARY

The Ezcurra Inlet, where the investigations were carried out during the Antarctic summer, fairly typical for Arctic and Antarctic waters, con-

stitutes deep water body with a limited inflow of oceanic water, surrounded by a glacier. The optical parameters measured differed greatly. The structure of this variability is highly complex: distinct and rapid fluctuations, very irregular, with hourly periods and minor tidal effects together with long oscillations, with ten-day periods were noted. The analysis of temporal variation of the values averaged within 10-day intervals made it possible to detect a strong maximum in the coefficient of beam attenuation in the second decade of the investigations (1977-12-30 through 1978-1—9), in the entire range of depths, and accompanied by a local maximum in the coefficient of irradiance attenuation in the euphotic zone, with a pronounced minimum in the third and fourth decade (1978-1-9 through 1978-1-29), coupled with a local minimum in the coefficient of beam attenuation at the surface, moving towards the fourth and fifth decade (1978-01-19 through 1978-02-08) with increasing depth. An independent analysis of the first and second halves of the investigations showed an increase in the coefficients of beam attenuation and irradiance attenuation, as well as albedo of scattering in the surface layer (0 to 20 m) that occurred in the second half (1978-01-29 through 1978-03-10) related, most probably, with an increase in the concentration of light-scattering inorganic matter. It is worthwhile mentioning that a simultaneous decrease in the mean coefficient of beam attenuation was observed at greater depths (30 to 70 m), which might have been due to the more intensive influx of clear oceanic water. Thus, water layer with an unchanged mean value of the coefficient of beam attenuation must have been present at transient depths (15 to 30 m) in the first and second halves of the investigations.

As only one cycle of investigations was carried out, it is difficult to ascertain whether the temporal changes presented here are typical for the environment investigated. The characteristics obtained from joint analysis of all data obtained during the investigations could be considered to be more typical. This analysis offers several major conclusions, of which the most important can be assumed to be that the attenuation of light in waters studied is primarily caused by scattering of light in suspended inorganic matter. The contribution of absorption in dissolved yellow organic substance is negligible, much smaller than in the Baltic, which must be due to small concentrations of this substance, in the presence of highly concentrated inorganic suspensions.

Instantaneous vertical profiles at the measuring stations indicate considerable horizontal stratification of water, as regards the coefficient of beam attenuation, which has been shown to be primarily related to the concentration of inorganic suspensions. A distinct layer of more turbid water, with a high coefficient of attenuation was detected in most

cases at the water surface, while clear or very clear water was present in the bottom layer. Since the boundaries of these layers vary with time, they become smeared in the average profile, the strong increase in clarity of water with depth becomes more pronounced, from the surface to about 30 m, while a certain stabilization of clarity is observed in the 30-m bottom layer. The interval of relative variation of the coefficient of attenuation in the vertical profile is fairly smooth, except for a certain minimum stability at a depth of about 40 to 60 m and the maximum some 5 to 10 m below the surface and at the sea bed.

In spite of considerable magnitudes of the total coefficient of beam attenuation, particularly close to the surface, the waters of the investigated environment have a fairly thick euphotic zone. The average thickness, throughout the entire period of investigations, can be estimated as 24 m, while the most typical figures for the Baltic are usually about 20 m, with the coefficients c much smaller than those in the Ezcurra Inlet. This interesting property is connected with extremely high scattering in the overall process of light attenuation, apparently the most typical optical property of the investigated area.

Jerzy OLSZEWSKI

Polska Akademia Nauk
Zakład Oceanologii w Sopocie

PODSTAWOWE WŁASNOŚCI OPTYCZNE WODY FIORDU EZCURRA

Streszczenie

Artykuł przedstawia wyniki części badań optycznych prowadzonych podczas II Polskiej Wyprawy Antarktycznej od 20 XII 1977 do 10 III 1978 r. we fiordzie Ezcurra. Badania miały na celu określenie typowych wartości oraz przedziałów zmienności współczynników: osłabiania wiązki promieni c oraz dyfuzyjnego osłabiania oświetlenia odgórnego k_d. Wyniki pomiarów tych współczynników przedstawiono tabelarycznie.

Analizując przedstawione w tabelach wyniki dla długości fali świetlnej 525 nm stwierdzono silną i nieregularną zmienność czasową badanych parametrów, zarówno w okresach krótkich (do godziny — rys. 1, 2), jak i w okresach dłuższych (10-dniowych — rys. 3, 9), przy czym w drugiej połowie badań stwierdzono wzrost średnich wartości tych parametrów w strefie eufotycznej. Znaleziony dla całego okresu ba-

dań średni profil pionowy współczynnika osłabiania wiązki, wraz z odpowiednimi, przybliżonymi wyrażeniem 2, rozkładami gęstości prawdopodobieństwa (rys. 4, 5) wykazuje silny spadek wartości tego współczynnika z głębokością od 1,29 m^{-1} przy powierzchni do 0.76 na głębokości 30 m, poniżej której zmiany c stają się nieznaczne (0.76 ± 0.03 m^{-1}).

W toku dalszej analizy stwierdzono dobrą liniową korelację pomiędzy współczynnikami osłabiania zarówno wiązki światła (rys. 6, 7, wz. 3) jak i oświetlenia (rys. 13, wz. 7) dla trzech długości fali świetlnej (425, 525, 600 nm), co pozwoliło m. in. odtworzyć, przybliżony wyrażeniem 4, średni kształt pełnego widma współczynnika osłabiania wiązki (rys. 8). Zasadniczą cechą wyróżniającą odtworzone widmo w porównaniu z przykładowo pokazanym na rys. 8 widmem c dla Bałtyku jest wyraźnie słabszy wzrost c ze spadkiem długości fali świetlnej i pewne przesunięcie minimum przebiegu w stronę fal krótkich. Taki przebieg można tłumaczyć znacznie mniejszą niż w Bałtyku zawartością rozpuszczonych w wodzie żółtych substancji pochodzenia organicznego i odpowiednio większą koncentracją zawiesin nieorganicznych.

Wniosek ten potwierdzają badania współczynnika osłabiania oświetlenia i związanego z nim zasięgu strefy eufotycznej (wz. 5). Wobec zaobserwowanych dużych wartości współczynnika osłabiania wiązki blisko powierzchni stwierdzono wyjątkowo duży, rzędu 24 m, zasięg strefy eufotycznej (rys. 9). Wiąże się to właśnie z dużym, ok. 80% (rys. 14), udziałem rozpraszania na zawiesinach w całkowitym procesie osłabiania światła. Tę ostatnią cechę optyczną można uznać za najbardziej charakterystyczną dla wód badanego akwenu.

REFERENCES

1. Dera, J.: *Charakterystyka oświetlenia strefy eufotycznej w morzu*, Oceanologia 1971, 1, 9.
2. Dera, J., J. Olszewski: *Widzialność podwodna*, Postępy Fizyki 1969, 20, 473.
3. Gerchun, A. A.: *K teorii svetovovo polya v rasseivayuschei srede*, DAN SSSR 1945, 49, 8.
4. Hale, G. M., M. R. Querry: *Optical constant of water in the 200-nm to 200-μm wavelength region*. Appl. Opt. 1973, 12, 525.
5. Ivanov, A. P.: *Fizicheskie osnovy gidrooptiki*, Mińsk 1975.
6. Jerlov, N. G.: *Marine optics*, Elsevier Oceanography Series, 14, Amsterdam — Oxford — New York 1976.
7. Kalle, K.: *The problem of the Gelbstoff in the sea*, Oceanogr. Mar. Biol. Ann. 1966, 4, 91.
8. Lundgren, B.: *Spectral transmittance measurements in the Baltic*, Rep. Univ. Copenhagen 1976, rep. 30.
9. Olszewski, J.: *Analiza warunków widzialności podwodnej w morzu na przykładzie Zatoki Gdańskiej*, Oceanologia 1973, 2, 153.
10. Preisendorfer, R. W.: *Application of radiative transfer theory to light measurements in the sea*, JUGG Monogr. 1961, 10, 83.

11. Woźniak, B., K. Montwiłł: *Metody i techniki pomiarów optycznych w morzu*, Stud. Mater. Oceanalog. KBM PAN 1973, 7, 73.
12. Woźniak, B.: *Nowe rezultaty badań udziału procesów absorpcji i rozpraszania w całkowitym osłabianiu światła w wodach bałtyckich*, Stud. Mater. Oceanolog. KBM PAN 1977, 19, 90.
13. Woźniak, B., R. Hapter, B. Maj: *The inflow of solar energy and the irradiance of the euphotic zone in the region of Ezcurra Inlet during the antarctic summer of 1977/78*, Oceanologia, 1983, 15.

Manuscript received in 1979